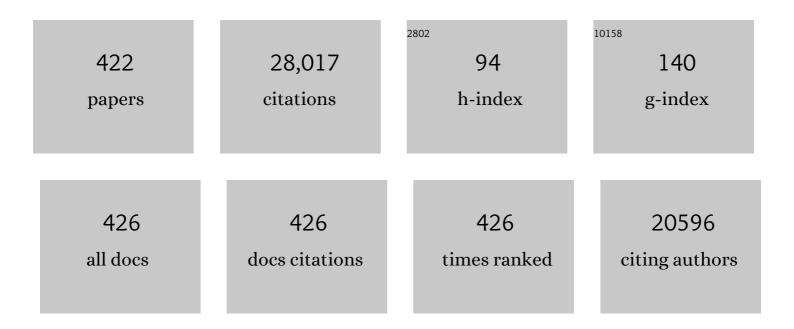
List of Publications by Year in descending order

Source: https://exaly.com/author-pdf/4472784/publications.pdf Version: 2024-02-01



Υίται Οιάν

| # | Article | IF | CITATIONS |
|----|--|------|-----------|
| 1 | Molten-LiCl induced thermochemical prelithiation of SiOx: Regulating the active Si/O ratio for high initial Coulombic efficiency. Nano Research, 2022, 15, 230-237. | 10.4 | 31 |
| 2 | A Friendly Soluble Protic Additive Enabling High Discharge Capability and Stabilizing Li Metal Anodes in Li–O ₂ Batteries. Advanced Functional Materials, 2022, 32, 2106984. | 14.9 | 13 |
| 3 | Rational Design of Tungsten Selenide @ Nâ€Doped Carbon Nanotube for Highâ€&table Potassiumâ€lon Batteries. Small, 2022, 18, e2104363. | 10.0 | 20 |
| 4 | Single-atom catalyst cathodes for lithium–oxygen batteries: a review. Nano Futures, 2022, 6, 012002. | 2.2 | 4 |
| 5 | Zeroâ€Strain Structure for Efficient Potassium Storage: Nitrogenâ€Enriched Carbon Dualâ€Confinement CoP Composite. Advanced Energy Materials, 2022, 12, 2103341. | 19.5 | 26 |
| 6 | Understanding electrolyte salt chemistry for advanced potassium storage performances of transitionâ€metal sulfides. , 2022, 4, 332-345. | | 10 |
| 7 | Petroleum coke derived porous carbon/NiCoP with efficient reviving catalytic and adsorptive activity as sulfur host for high performance lithium—sulfur batteries. Nano Research, 2022, 15, 4058-4067. | 10.4 | 10 |
| 8 | Unravelling binder chemistry in sodium/potassium ion batteries for superior electrochemical performances. Journal of Materials Chemistry A, 2022, 10, 4060-4067. | 10.3 | 25 |
| 9 | Cationâ€Dependent Hydrogel Templateâ€Activation Strategy: Constructing 3D Anode and High Specific Surface Cathode for Dualâ€Carbon Potassiumâ€Ion Hybrid Capacitor. Small, 2022, 18, e2106712. | 10.0 | 7 |
| 10 | One-Step, Vacuum-Assisted Construction of Micrometer-Sized Nanoporous Silicon Confined by Uniform Two-Dimensional N-Doped Carbon toward Advanced Li Ion and MXene-Based Li Metal Batteries. ACS Nano, 2022, 16, 4560-4577. | 14.6 | 75 |
| 11 | Hierarchical Ion/Electron Networks Enable Efficient Red Phosphorus Anode with High Mass Loading for Sodium Ion Batteries. Advanced Functional Materials, 2022, 32, . | 14.9 | 21 |
| 12 | Space-confined growth of Bi2Se3 nanosheets encapsulated in N-doped carbon shell lollipop-like composite for full/half potassium-ion and lithium-ion batteries. Nano Today, 2022, 43, 101408. | 11.9 | 30 |
| 13 | Site-Selective Adsorption on ZnF ₂ /Ag Coated Zn for Advanced Aqueous Zinc–Metal Batteries at Low Temperature. Nano Letters, 2022, 22, 1750-1758. | 9.1 | 95 |
| 14 | MXenes and their derivatives for advanced aqueous rechargeable batteries. Materials Today, 2022, 52, 225-249. | 14.2 | 39 |
| 15 | Bimetallic Bi–Sn microspheres as high initial coulombic efficiency and long lifespan anodes for sodium-ion batteries. Chemical Communications, 2022, 58, 5140-5143. | 4.1 | 15 |
| 16 | Intercalation of organics into layered structures enables superior interface compatibility and fast charge diffusion for dendrite-free Zn anodes. Energy and Environmental Science, 2022, 15, 1682-1693. | 30.8 | 105 |
| 17 | Iron Selenideâ€Based Heterojunction Construction and Defect Engineering for Fast Potassium/Sodiumâ€lon Storage. Small, 2022, 18, e2107252. | 10.0 | 46 |
| 18 | Controlled Tin Oxide Nanoparticles Encapsulated in N-Doped Carbon Nanofibers for Superior Lithium-Ion Storage. ACS Applied Energy Materials, 2022, 5, 1840-1848. | 5.1 | 4 |

| # | Article | IF | CITATIONS |
|----|---|------|-----------|
| 19 | Manipulating Electrocatalytic Polysulfide Redox Kinetics by 1D Core–Shell Like Composite for Lithium–Sulfur Batteries. Advanced Energy Materials, 2022, 12, . | 19.5 | 47 |
| 20 | Bipolar electrode architecture enables high-energy aqueous rechargeable sodium ion battery. Nano Research, 2022, 15, 5072-5080. | 10.4 | 7 |
| 21 | Niobium Diboride Nanoparticles Accelerating Polysulfide Conversion and Directing Li ₂ S Nucleation Enabled High Areal Capacity Lithium–Sulfur Batteries. ACS Nano, 2022, 16, 4947-4960. | 14.6 | 88 |
| 22 | Highly Reversible Zn Metal Anodes Enabled by Freestanding, Lightweight, and Zincophilic MXene/Nanoporous Oxide Heterostructure Engineered Separator for Flexible Zn-MnO ₂ Batteries. ACS Nano, 2022, 16, 6755-6770. | 14.6 | 103 |
| 23 | Towards Highâ€Performance Aqueous Sodium Ion Batteries: Constructing Hollow NaTi ₂ (PO ₄) ₃ @C Nanocube Anode with Zn Metalâ€Induced Preâ€Sodiation and Deep Eutectic Electrolyte. Advanced Energy Materials, 2022, 12, . | 19.5 | 30 |
| 24 | Highly reversible Mg metal anodes enabled by interfacial liquid metal engineering for high-energy Mg-S batteries. Energy Storage Materials, 2022, 48, 447-457. | 18.0 | 46 |
| 25 | Highly reversible and safe lithium metal batteries enabled by Non-flammable All-fluorinated carbonate electrolyte conjugated with 3D flexible MXene-based lithium anode. Chemical Engineering Journal, 2022, 440, 135818. | 12.7 | 23 |
| 26 | Chemical Buffer Layer Enabled Highly Reversible Zn Anode for Deeply Discharging and Long‣ife Zn–Air Battery. Small, 2022, 18, e2106604. | 10.0 | 16 |
| 27 | Synthesis of carbon nanotubes-supported porous silicon microparticles in low-temperature molten salt for high-performance Li-ion battery anodes. Nano Research, 2022, 15, 6184-6191. | 10.4 | 22 |
| 28 | Review of room-temperature liquid metals for advanced metal anodes in rechargeable batteries. Energy Storage Materials, 2022, 50, 473-494. | 18.0 | 35 |
| 29 | Constructing Reactive Microâ€Environment in Basal Plane of MoS ₂ for pHâ€Universal Hydrogen Evolution Catalysis. Small, 2022, 18, . | 10.0 | 21 |
| 30 | Electron-redistributed Ni–Co oxide nanoarrays as an ORR/OER bifunctional catalyst for low overpotential and long lifespan Li–O ₂ batteries. Journal of Materials Chemistry A, 2022, 10, 14613-14621. | 10.3 | 12 |
| 31 | MXenes for advanced separator in rechargeable batteries. Materials Today, 2022, 57, 146-179. | 14.2 | 38 |
| 32 | One-pot synthesis of uniform MoSe2 nanoparticles as high performance anode materials for lithium/sodium ion batteries. Journal of Alloys and Compounds, 2022, 922, 166306. | 5.5 | 15 |
| 33 | Stable and dendrite-free lithium metal anodes enabled by carbon paper incorporated with ultrafine lithiophilic TiO2 derived from MXene and carbon dioxide. Chemical Engineering Journal, 2021, 406, 126836. | 12.7 | 45 |
| 34 | Improved Na storage and Coulombic efficiency in TiP2O7@C microflowers for sodium ion batteries. Nano Research, 2021, 14, 139-147. | 10.4 | 18 |
| 35 | Interfacial passivation by room-temperature liquid metal enabling stable 5 V-class lithium-metal batteries in commercial carbonate-based electrolyte. Energy Storage Materials, 2021, 34, 12-21. | 18.0 | 85 |
| 36 | 2D interspace confined growth of ultrathin MoS2-intercalated graphite hetero-layers for high-rate Li/K storage_Nano Research_2021_14_1061-1068 | 10.4 | 19 |

| # | Article | IF | CITATIONS |
|----|--|-------------|-----------|
| 37 | Revealing the Doubleâ€Edged Behaviors of Heteroatom Sulfur in Carbonaceous Materials for Balancing Kâ€Storage Capacity and Stability. Advanced Functional Materials, 2021, 31, 2006875. | 14.9 | 42 |
| 38 | Recent Advances and Perspectives of Znâ€Metal Free "Rockingâ€Chairâ€â€Type Znâ€lon Batteries. Advanced Energy Materials, 2021, 11, 2002529. | 19.5 | 111 |
| 39 | Quantumâ€Matter Bi/TiO ₂ Heterostructure Embedded in Nâ€Doped Porous Carbon Nanosheets for Enhanced Sodium Storage. Small Structures, 2021, 2, 2000085. | 12.0 | 77 |
| 40 | Hierarchical interlayer-expanded MoSe ₂ /N–C nanorods for high-rate and long-life sodium and potassium-ion batteries. Inorganic Chemistry Frontiers, 2021, 8, 1271-1278. | 6.0 | 22 |
| 41 | Carbon coated SiO nanoparticles embedded in hierarchical porous N-doped carbon nanosheets for enhanced lithium storage. Inorganic Chemistry Frontiers, 2021, 8, 4282-4290. | 6.0 | 18 |
| 42 | Yolk–shell structured CoSe ₂ /C nanospheres as multifunctional anode materials for both full/half sodium-ion and full/half potassium-ion batteries. Nanoscale, 2021, 13, 10385-10392. | 5.6 | 36 |
| 43 | A porous polycrystalline NiCo ₂ P _{<i>x</i>} as a highly efficient host for sulfur cathodes in Li–S batteries. Journal of Materials Chemistry A, 2021, 9, 23149-23156. | 10.3 | 19 |
| 44 | An aqueous rechargeable lithium ion battery with long cycle life and overcharge self-protection. Materials Chemistry Frontiers, 2021, 5, 2749-2757. | 5.9 | 9 |
| 45 | Rocking Chair Batteries: Recent Advances and Perspectives of Znâ€Metal Free "Rockingâ€Chairâ€â€Type Znâ€ Batteries (Adv. Energy Mater. 5/2021). Advanced Energy Materials, 2021, 11, 2170023. | lon 19.5 | 3 |
| 46 | Applications of MoS ₂ in Li–O ₂ Batteries: Development and Challenges. Energy & Fuels, 2021, 35, 5613-5626. | 5.1 | 20 |
| 47 | Dandelion-Like Bi2S3/rGO hierarchical microspheres as high-performance anodes for potassium-ion and half/full sodium-ion batteries. Nano Research, 2021, 14, 4696-4703. | 10.4 | 39 |
| 48 | Dealloying: An effective method for scalable fabrication of 0D, 1D, 2D, 3D materials and its application in energy storage. Nano Today, 2021, 37, 101094. | 11.9 | 93 |
| 49 | Molten Salt Derived <scp>Grapheneâ€Like</scp> Carbon Nanosheets Wrapped <scp>SiO_{<i>x</i>}</scp> /Carbon Submicrospheres with Enhanced Lithium Storage ^{â€} . Chinese Journal of Chemistry, 2021, 39, 1233-1239. | 4.9 | 9 |
| 50 | Hydrothermal "Disproportionation―of Biomass into Oriented Carbon Microsphere Anode and 3D Porous Carbon Cathode for Potassium Ion Hybrid Capacitor. Advanced Functional Materials, 2021, 31, 2103115. | 14.9 | 49 |
| 51 | Revealing Quasi-1D Volume Expansion in Na-/K-Ion Battery Anodes: A Case Study of Sb ₂ O ₃ Microbelts. CCS Chemistry, 2021, 3, 1306-1315. | 7.8 | 17 |
| 52 | Stable Aqueous Anodeâ€Free Zinc Batteries Enabled by Interfacial Engineering. Advanced Functional Materials, 2021, 31, 2101886. | 14.9 | 162 |
| 53 | Highâ€Voltage and Superâ€Stable Aqueous Sodium–Zinc Hybrid Ion Batteries Enabled by Double Solvation Structures in Concentrated Electrolyte. Small Methods, 2021, 5, e2100418. | 8.6 | 22 |
| 54 | Coordinatively and Spatially Coconfining High-Loading Atomic Sb in Sulfur-Rich 2D Carbon Matrix for | | 10 |

Fast K⁺ Diffusion and Storage., 2021, 3, 790-798.

| # | Article | IF | CITATIONS |
|----|--|------|-----------|
| 55 | Design of safe, long-cycling and high-energy lithium metal anodes in all working conditions: Progress, challenges and perspectives. Energy Storage Materials, 2021, 38, 157-189. | 18.0 | 52 |
| 56 | Scalable and Controllable Synthesis of Interface-Engineered Nanoporous Host for Dendrite-Free and High Rate Zinc Metal Batteries. ACS Nano, 2021, 15, 11828-11842. | 14.6 | 140 |
| 57 | Construction and electrochemical mechanism investigation of hierarchical core—shell like composite as high performance anode for potassium ion batteries. Nano Research, 2021, 14, 3552-3561. | 10.4 | 21 |
| 58 | Rational Design of Sulfur-Doped Three-Dimensional Ti ₃ C ₂ T <i>_{<i>x</i>}</i> MXene/ZnS Heterostructure as Multifunctional Protective Layer for Dendrite-Free Zinc-Ion Batteries. ACS Nano, 2021, 15, 15259-15273. | 14.6 | 167 |
| 59 | Covalent Organic Frameworks and Their Derivatives for Better Metal Anodes in Rechargeable Batteries. ACS Nano, 2021, 15, 12741-12767. | 14.6 | 71 |
| 60 | Reversible zinc-based anodes enabled by zincophilic antimony engineered MXene for stable and dendrite-free aqueous zinc batteries. Energy Storage Materials, 2021, 41, 343-353. | 18.0 | 145 |
| 61 | Regulating polysulfide intermediates by ultrathin Co-Bi nanosheet electrocatalyst in lithiumâ^'sulfur batteries. Nano Today, 2021, 40, 101246. | 11.9 | 34 |
| 62 | Ultra-long-life and highly reversible Zn metal anodes enabled by a desolvation and deanionization interface layer. Energy and Environmental Science, 2021, 14, 3120-3129. | 30.8 | 250 |
| 63 | A large format aqueous rechargeable LiMn2O4/Zn battery with high energy density and long cycle life. Science China Materials, 2021, 64, 783-788. | 6.3 | 12 |
| 64 | Rational fabrication of CoS2/Co4S3@N-doped carbon microspheres as excellent cycling performance anode for half/full sodium ion batteries. Energy Storage Materials, 2020, 25, 679-686. | 18.0 | 111 |
| 65 | Self-wrinkled graphene as a mechanical buffer: A rational design to boost the K-ion storage performance of Sb2Se3 nanoparticles. Chemical Engineering Journal, 2020, 379, 122352. | 12.7 | 49 |
| 66 | Isotropic Li nucleation and growth achieved by an amorphous liquid metal nucleation seed on MXene framework for dendrite-free Li metal anode. Energy Storage Materials, 2020, 26, 223-233. | 18.0 | 100 |
| 67 | Rational design of polar/nonpolar mediators toward efficient sulfur fixation and enhanced conductivity. Journal of Materials Chemistry A, 2020, 8, 1010-1051. | 10.3 | 32 |
| 68 | Porosity―and Graphitization ontrolled Fabrication of Nanoporous Silicon@Carbon for Lithium Storage and Its Conjugation with MXene for Lithiumâ€Metal Anode. Advanced Functional Materials, 2020, 30, 1908721. | 14.9 | 159 |
| 69 | High-Spin Sulfur-Mediated Phosphorous Activation Enables Safe and Fast Phosphorus Anodes for Sodium-Ion Batteries. CheM, 2020, 6, 221-233. | 11.7 | 43 |
| 70 | N-induced lattice contraction generally boosts the hydrogen evolution catalysis of P-rich metal phosphides. Science Advances, 2020, 6, eaaw8113. | 10.3 | 211 |
| 71 | Orbital-regulated interfacial electronic coupling endows Ni3N with superior catalytic surface for hydrogen evolution reaction. Science China Chemistry, 2020, 63, 1563-1569. | 8.2 | 22 |
| 72 | Recently advances and perspectives of anode-free rechargeable batteries. Nano Energy, 2020, 78, 105344. | 16.0 | 108 |

| # | Article | IF | CITATIONS |
|----|--|------|-----------|
| 73 | Two-Dimensional Silicon/Carbon from Commercial Alloy and CO ₂ for Lithium Storage and Flexible Ti ₃ C ₂ T _{<i>x</i>} MXene-Based Lithium–Metal Batteries. ACS Nano, 2020, 14, 17574-17588. | 14.6 | 108 |
| 74 | Guiding Smooth Li Plating and Stripping by a Spherical Island Model for Lithium Metal Anodes. ACS Applied Materials & Interfaces, 2020, 12, 38098-38105. | 8.0 | 17 |
| 75 | Recent advances and perspectives of 2D silicon: Synthesis and application for energy storage and conversion. Energy Storage Materials, 2020, 32, 115-150. | 18.0 | 74 |
| 76 | Ultrahigh-Areal-Capacity Battery Anodes Enabled by Free-Standing Vanadium Nitride@N-Doped Carbon/Graphene Architecture. ACS Applied Materials & Interfaces, 2020, 12, 49607-49616. | 8.0 | 24 |
| 77 | Nanoribbon Superstructures of Graphene Nanocages for Efficient Electrocatalytic Hydrogen Evolution. Nano Letters, 2020, 20, 7342-7349. | 9.1 | 30 |
| 78 | Defect engineering on carbon black for accelerated Li-S chemistry. Nano Research, 2020, 13, 3315-3320. | 10.4 | 52 |
| 79 | Aqueous Rechargeable Li ⁺ /Na ⁺ Hybrid Ion Battery with High Energy Density and Long Cycle Life. Small, 2020, 16, e2003585. | 10.0 | 16 |
| 80 | Porous lithium cobalt oxide fabricated from metal–organic frameworks as a high-rate cathode for lithium-ion batteries. RSC Advances, 2020, 10, 31889-31893. | 3.6 | 4 |
| 81 | NaTi ₂ (PO ₄) ₃ Solidâ€State Electrolyte Protection Layer on Zn Metal Anode for Superior Longâ€Life Aqueous Zincâ€lon Batteries. Advanced Functional Materials, 2020, 30, 2004885. | 14.9 | 115 |
| 82 | Recent Advances of Emerging 2D MXene for Stable and Dendriteâ€Free Metal Anodes. Advanced Functional Materials, 2020, 30, 2004613. | 14.9 | 140 |
| 83 | Phosphorus-doped hard carbon with controlled active groups and microstructure for high-performance sodium-ion batteries. Journal of Materials Chemistry A, 2020, 8, 20486-20492. | 10.3 | 33 |
| 84 | Kirkendall effect modulated hollow red phosphorus nanospheres for high performance sodium-ion battery anodes. Chemical Communications, 2020, 56, 11795-11798. | 4.1 | 17 |
| 85 | Chemical fixation of CO2 on activated Si: Producing graphitic carbon-stabilized Si particles for Li-storage. Energy Storage Materials, 2020, 31, 36-43. | 18.0 | 11 |
| 86 | N-Doped carbon nanotubes decorated with Fe/Ni sites to stabilize lithium metal anodes. Inorganic Chemistry Frontiers, 2020, 7, 2747-2752. | 6.0 | 12 |
| 87 | A Highâ€Energy and Longâ€Life Aqueous Zn/Birnessite Battery via Reversible Water and Zn ²⁺ Coinsertion. Small, 2020, 16, e2001228. | 10.0 | 75 |
| 88 | Heteroatom-doped 3D porous carbon architectures for highly stable aqueous zinc metal batteries and non-aqueous lithium metal batteries. Chemical Engineering Journal, 2020, 400, 125843. | 12.7 | 115 |
| 89 | Boosting Zinc-Ion Storage Capability by Effectively Suppressing Vanadium Dissolution Based on Robust Layered Barium Vanadate. Nano Letters, 2020, 20, 2899-2906. | 9.1 | 208 |
| 90 | Hierarchical Fusiform Microrods Constructed by Parallelly Arranged Nanoplatelets of LiCoO ₂ Material with Ultrahigh Rate Performance. ACS Applied Materials & Interfaces, 2020, 12, 17376-17384. | 8.0 | 9 |

| # | Article | IF | CITATIONS |
|-----|--|----------------------------|-------------|
| 91 | Promoting spherical epitaxial deposition of solid sulfides for high-capacity Li–S batteries. Journal of Materials Chemistry A, 2020, 8, 7100-7108. | 10.3 | 10 |
| 92 | Conductive cobalt doped niobium nitride porous spheres as an efficient polysulfide convertor for advanced lithium-sulfur batteries. Journal of Materials Chemistry A, 2020, 8, 6276-6282. | 10.3 | 58 |
| 93 | Electrolyte solvation structure manipulation enables safe and stable aqueous sodium ion batteries. Journal of Materials Chemistry A, 2020, 8, 14190-14197. | 10.3 | 42 |
| 94 | Dual taming of polysufides by phosphorus-doped carbon for improving electrochemical performances of lithium–sulfur battery. Electrochimica Acta, 2020, 354, 136648. | 5.2 | 40 |
| 95 | Nanoporous Si@Carbon: Porosity―and Graphitizationâ€Controlled Fabrication of Nanoporous Silicon@Carbon for Lithium Storage and Its Conjugation with MXene for Lithiumâ€Metal Anode (Adv.) Tj ETQq1 J | 0 <i>4</i> 7. 0 431 | 4 ₂gBT /Ove |
| 96 | Carbon-coated mesoporous Co9S8 nanoparticles on reduced graphene oxide as a long-life and high-rate anode material for potassium-ion batteries. Nano Research, 2020, 13, 802-809. | 10.4 | 61 |
| 97 | Construction of hierarchical MoSe ₂ @C hollow nanospheres for efficient lithium/sodium ion storage. Inorganic Chemistry Frontiers, 2020, 7, 1691-1698. | 6.0 | 22 |
| 98 | Silicothermic reduction reaction for fabricating interconnected Si–Ge nanocrystals with fast and stable Li-storage. Journal of Materials Chemistry A, 2020, 8, 6597-6606. | 10.3 | 19 |
| 99 | Formation of Solid–Electrolyte Interfaces in Aqueous Electrolytes by Altering Cationâ€Solvation Shell Structure. Advanced Energy Materials, 2020, 10, 1903665. | 19.5 | 59 |
| 100 | Stable Lithium Deposition Enabled by an Acid-Treated g-C ₃ N ₄ Interface Layer for a Lithium Metal Anode. ACS Applied Materials & Interfaces, 2020, 12, 11265-11272. | 8.0 | 24 |
| 101 | Amidationâ€Dominated Reâ€Assembly Strategy for Singleâ€Atom Design/Nanoâ€Engineering: Constructing Ni/S/C Nanotubes with Fast and Stable Kâ€Storage. Angewandte Chemie - International Edition, 2020, 59, 6459-6465. | 13.8 | 23 |
| 102 | Amidationâ€Dominated Reâ€Assembly Strategy for Singleâ€Atom Design/Nanoâ€Engineering: Constructing Ni/S/C Nanotubes with Fast and Stable Kâ€Storage. Angewandte Chemie, 2020, 132, 6521-6527. | 2.0 | 1 |
| 103 | ZIF-Derived Cobalt-Containing N-Doped Carbon-Coated SiO _{<i>x</i>} Nanoparticles for Superior Lithium Storage. ACS Applied Materials & Interfaces, 2020, 12, 7206-7211. | 8.0 | 43 |
| 104 | Micron-Sized Nanoporous Vanadium Pentoxide Arrays for High-Performance Gel Zinc-Ion Batteries and Potassium Batteries. Chemistry of Materials, 2020, 32, 4054-4064. | 6.7 | 105 |
| 105 | Regulating the Interfacial Electronic Coupling of Fe ₂ N via Orbital Steering for Hydrogen Evolution Catalysis. Advanced Materials, 2020, 32, e1904346. | 21.0 | 86 |
| 106 | Recent advances and perspectives in stable and dendrite-free potassium metal anodes. Energy Storage Materials, 2020, 30, 206-227. | 18.0 | 95 |
| 107 | Appropriately hydrophilic/hydrophobic cathode enables high-performance aqueous zinc-ion batteries. Energy Storage Materials, 2020, 30, 337-345. | 18.0 | 92 |
| 108 | Edge-Plane Exposed N-Doped Carbon Nanofibers Toward Fast K-Ion Adsorption/Diffusion Kinetics for K-Ion Capacitors. CCS Chemistry, 2020, 2, 495-506. | 7.8 | 17 |

| # | Article | IF | CITATIONS |
|-----|---|------|-----------|
| 109 | A flexible micro/nanostructured Si microsphere cross-linked by highly-elastic carbon nanotubes toward enhanced lithium ion battery anodes. Energy Storage Materials, 2019, 17, 93-100. | 18.0 | 113 |
| 110 | An Al ₂ O ₃ coating layer on mesoporous Si nanospheres for stable solid electrolyte interphase and high-rate capacity for lithium ion batteries. Nanoscale, 2019, 11, 16781-16787. | 5.6 | 22 |
| 111 | Uniform Li deposition by regulating the initial nucleation barrier <i>via</i> a simple liquid-metal coating for a dendrite-free Li–metal anode. Journal of Materials Chemistry A, 2019, 7, 18861-18870. | 10.3 | 93 |
| 112 | Rechargeable aqueous hybrid ion batteries: developments and prospects. Journal of Materials Chemistry A, 2019, 7, 18708-18734. | 10.3 | 128 |
| 113 | Porosity controlled synthesis of nanoporous silicon by chemical dealloying as anode for high energy lithium-ion batteries. Journal of Colloid and Interface Science, 2019, 554, 674-681. | 9.4 | 38 |
| 114 | Layered (NH ₄) ₂ V ₆ O ₁₆ ·1.5H ₂ O nanobelts as a high-performance cathode for aqueous zinc-ion batteries. Journal of Materials Chemistry A, 2019, 7, 19130-19139. | 10.3 | 121 |
| 115 | In Situ Revealing the Electroactivity of PO and PC Bonds in Hard Carbon for Highâ€Capacity and Longâ€Life Li/Kâ€lon Batteries. Advanced Energy Materials, 2019, 9, 1901676. | 19.5 | 202 |
| 116 | Waterâ€Induced Growth of a Highly Oriented Mesoporous Graphitic Carbon Nanospring for Fast Potassiumâ€Ion Adsorption/Intercalation Storage. Angewandte Chemie, 2019, 131, 18276-18283. | 2.0 | 16 |
| 117 | Waterâ€Induced Growth of a Highly Oriented Mesoporous Graphitic Carbon Nanospring for Fast Potassiumâ€Ion Adsorption/Intercalation Storage. Angewandte Chemie - International Edition, 2019, 58, 18108-18115. | 13.8 | 106 |
| 118 | Roomâ€Temperature Liquid Metal Confined in MXene Paper as a Flexible, Freestanding, and Binderâ€Free Anode for Nextâ€Generation Lithiumâ€Ion Batteries. Small, 2019, 15, e1903214. | 10.0 | 79 |
| 119 | Scalable and Physical Synthesis of 2D Silicon from Bulk Layered Alloy for Lithium-Ion Batteries and Lithium Metal Batteries. ACS Nano, 2019, 13, 13690-13701. | 14.6 | 143 |
| 120 | Co0.85Se hollow spheres constructed of ultrathin 2D mesoporous nanosheets as a novel bifunctional-electrode for supercapacitor and water splitting. Nano Research, 2019, 12, 2941-2946. | 10.4 | 25 |
| 121 | Green and tunable fabrication of graphene-like N-doped carbon on a 3D metal substrate as a binder-free anode for high-performance potassium-ion batteries. Journal of Materials Chemistry A, 2019, 7, 21966-21975. | 10.3 | 48 |
| 122 | Converting Waste Polyethylene into ZnCCo ₃ and ZnCNi ₃ by a One-Step Thermal Reduction Process. ACS Omega, 2019, 4, 15729-15733. | 3.5 | 11 |
| 123 | Passivation effect for current collectors enables high-voltage aqueous sodium ion batteries. Materials Today Energy, 2019, 14, 100337. | 4.7 | 32 |
| 124 | Flexible and Free-Standing Ti ₃ C ₂ T _{<i>x</i>} MXene@Zn Paper for Dendrite-Free Aqueous Zinc Metal Batteries and Nonaqueous Lithium Metal Batteries. ACS Nano, 2019, 13, 11676-11685. | 14.6 | 420 |
| 125 | Coral-like Ni _x Co _{1â^'x} Se ₂ for Na-ion battery with ultralong cycle life and ultrahigh rate capability. Journal of Materials Chemistry A, 2019, 7, 3933-3940. | 10.3 | 85 |
| 126 | Carbon nanotube-stabilized Co ₉ S ₈ dual-shell hollow spheres for high-performance K-ion storage. Chemical Communications, 2019, 55, 1406-1409. | 4.1 | 39 |

| # | Article | IF | CITATIONS |
|-----|---|------|-----------|
| 127 | Study on the effect of transition metal sulfide in lithium–sulfur battery. Inorganic Chemistry Frontiers, 2019, 6, 477-481. | 6.0 | 41 |
| 128 | In-situ rooting ZnSe/N-doped hollow carbon architectures as high-rate and long-life anode materials for half/full sodium-ion and potassium-ion batteries. Energy Storage Materials, 2019, 23, 35-45. | 18.0 | 189 |
| 129 | Meso-porous amorphous Ge: Synthesis and mechanism of an anode material for Na and K storage. Nano Research, 2019, 12, 1824-1830. | 10.4 | 22 |
| 130 | Double-Shelled Ni–Fe–P/N-Doped Carbon Nanobox Derived from a Prussian Blue Analogue as an Electrode Material for K-Ion Batteries and Li–S Batteries. ACS Energy Letters, 2019, 4, 1496-1504. | 17.4 | 138 |
| 131 | Polyanions Enhance Conversion Reactions for Lithium/Sodiumâ€ion Batteries: The Case of SbVO ₄ Nanoparticles on Reduced Graphene Oxide. Small Methods, 2019, 3, 1900231. | 8.6 | 31 |
| 132 | Amine-induced phase transition from white phosphorus to red/black phosphorus for Li/K-ion storage. Chemical Communications, 2019, 55, 6751-6754. | 4.1 | 22 |
| 133 | Self-templating growth of Sb ₂ Se ₃ @C microtube: a convention-alloying-type anode material for enhanced K-ion batteries. Journal of Materials Chemistry A, 2019, 7, 12283-12291. | 10.3 | 96 |
| 134 | Prelithiated Surface Oxide Layer Enabled High-Performance Si Anode for Lithium Storage. ACS Applied Materials & Interfaces, 2019, 11, 18305-18312. | 8.0 | 58 |
| 135 | Porous Si/C microspheres decorated with stable outer carbon interphase and inner interpenetrated Si@C channels for enhanced lithium storage. Carbon, 2019, 149, 664-671. | 10.3 | 49 |
| 136 | Water Splitting: Boosting Water Dissociation Kinetics on Pt–Ni Nanowires by Nâ€Induced Orbital Tuning (Adv. Mater. 16/2019). Advanced Materials, 2019, 31, 1970116. | 21.0 | 1 |
| 137 | A general method for constructing robust, flexible and freestanding MXene@metal anodes for high-performance potassium-ion batteries. Journal of Materials Chemistry A, 2019, 7, 9716-9725. | 10.3 | 162 |
| 138 | Hierarchical flower-like cobalt phosphosulfide derived from Prussian blue analogue as an efficient polysulfides adsorbent for long-life lithium-sulfur batteries. Nano Research, 2019, 12, 1115-1120. | 10.4 | 24 |
| 139 | Spatial separation of lithiophilic surface and superior conductivity for advanced Li metal anode: the case of acetylene black and N-doped carbon spheres. Journal of Materials Chemistry A, 2019, 7, 8765-8770. | 10.3 | 25 |
| 140 | Tuning orbital orientation endows molybdenum disulfide with exceptional alkaline hydrogen evolution capability. Nature Communications, 2019, 10, 1217. | 12.8 | 322 |
| 141 | Ultrathin mesoporous F-doped α-Ni(OH) ₂ nanosheets as an efficient electrode material for water splitting and supercapacitors. Journal of Materials Chemistry A, 2019, 7, 9656-9664. | 10.3 | 85 |
| 142 | Manipulating the water dissociation kinetics of Ni ₃ N nanosheets <i>via in situ</i> interfacial engineering. Journal of Materials Chemistry A, 2019, 7, 10924-10929. | 10.3 | 79 |
| 143 | Dendrite-tamed deposition kinetics using single-atom Zn sites for Li metal anode. Energy Storage Materials, 2019, 23, 587-593. | 18.0 | 73 |
| 144 | Sulfurâ€Deficient TiS _{2â€x} for Promoted Polysulfide Redox Conversion in Lithiumâ€Sulfur Batteries. ChemElectroChem, 2019, 6, 2231-2237. | 3.4 | 37 |

| # | Article | IF | CITATIONS |
|-----|---|------|-----------|
| 145 | Boosting Water Dissociation Kinetics on Pt–Ni Nanowires by Nâ€Induced Orbital Tuning. Advanced Materials, 2019, 31, e1807780. | 21.0 | 167 |
| 146 | New Insights into the Electrochemistry Superiority of Liquid Na–K Alloy in Metal Batteries. Small, 2019, 15, e1804916. | 10.0 | 26 |
| 147 | Pyridinic and pyrrolic nitrogen-enriched carbon as a polysulfide blocker for high-performance lithium–sulfur batteries. Inorganic Chemistry Frontiers, 2019, 6, 955-960. | 6.0 | 22 |
| 148 | One-step chemical synthesis of MgCNi3 nanoparticles embedded in carbon nanosheets utilizing waste polyethylene as carbon source. Materials Research Express, 2019, 6, 126003. | 1.6 | 3 |
| 149 | Hierarchical desert-waves-like LiNi0.5Mn1.5O4 as advanced cathodes with superior rate capability and cycling stability. Materials Today Energy, 2019, 14, 100363. | 4.7 | 11 |
| 150 | Enhancing kinetics of Li-S batteries by graphene-like N,S-codoped biochar fabricated in NaCl non-aqueous ionic liquid. Science China Materials, 2019, 62, 455-464. | 6.3 | 23 |
| 151 | Stabilizing antimony nanocrystals within ultrathin carbon nanosheets for high-performance K-ion storage. Energy Storage Materials, 2019, 20, 46-54. | 18.0 | 78 |
| 152 | Fully integrated hierarchical double-shelled Co ₉ S ₈ @CNT nanostructures with unprecedented performance for Li–S batteries. Nanoscale Horizons, 2019, 4, 182-189. | 8.0 | 62 |
| 153 | Mesoporous Hollow Ge Microspheres Prepared via Molten-Salt Metallothermic Reaction for High-Performance Li-Storage Anode. ACS Applied Materials & Interfaces, 2018, 10, 8399-8404. | 8.0 | 32 |
| 154 | Green, Scalable, and Controllable Fabrication of Nanoporous Silicon from Commercial Alloy Precursors for High-Energy Lithium-Ion Batteries. ACS Nano, 2018, 12, 4993-5002. | 14.6 | 269 |
| 155 | Sandwich-like Ni2P nanoarray/nitrogen-doped graphene nanoarchitecture as a high-performance anode for sodium and lithium ion batteries. Energy Storage Materials, 2018, 15, 234-241. | 18.0 | 179 |
| 156 | Self-Standing Hierarchical P/CNTs@rGO with Unprecedented Capacity and Stability for Lithium and Sodium Storage. CheM, 2018, 4, 372-385. | 11.7 | 128 |
| 157 | Manipulating the Redox Kinetics of Li–S Chemistry by Tellurium Doping for Improved Li–S Batteries. ACS Energy Letters, 2018, 3, 420-427. | 17.4 | 146 |
| 158 | Amorphous mesoporous GeO <i> _x </i> anode for Na-ion batteries with high capacity and long lifespan. Royal Society Open Science, 2018, 5, 171477. | 2.4 | 9 |
| 159 | Embedding MnO@Mn ₃ O ₄ Nanoparticles in an Nâ€Doped arbon Framework Derived from Mnâ€Organic Clusters for Efficient Lithium Storage. Advanced Materials, 2018, 30, 1704244. | 21.0 | 374 |
| 160 | Hierarchical Porous Nanosheets Constructed by Grapheneâ€Coated, Interconnected TiO ₂ Nanoparticles for Ultrafast Sodium Storage. Advanced Materials, 2018, 30, 1705788. | 21.0 | 247 |
| 161 | Ultrafine Co _{1â^'x} S nanoparticles embedded in a nitrogen-doped porous carbon hollow nanosphere composite as an anode for superb sodium-ion batteries and lithium-ion batteries. Nanoscale, 2018, 10, 2804-2811. | 5.6 | 69 |
| 162 | Sulfur–hydrazine hydrate-based chemical synthesis of sulfur@graphene composite for lithium–sulfur batteries. Inorganic Chemistry Frontiers, 2018, 5, 785-792. | 6.0 | 14 |

| # | Article | IF | CITATIONS |
|-----|---|------|-----------|
| 163 | Mesoporous germanium nanoparticles synthesized in molten zinc chloride at low temperature as a high-performance anode for lithium-ion batteries. Dalton Transactions, 2018, 47, 7402-7406. | 3.3 | 22 |
| 164 | Stabilizing Si/graphite composites with Cu and <i>in situ</i> synthesized carbon nanotubes for high-performance Li-ion battery anodes. Inorganic Chemistry Frontiers, 2018, 5, 1463-1469. | 6.0 | 38 |
| 165 | Synchronous synthesis of Kirkendall effect induced hollow FeSe ₂ /C nanospheres as anodes for high performance sodium ion batteries. Chemical Communications, 2018, 54, 5704-5707. | 4.1 | 89 |
| 166 | Solid-Solution Anion-Enhanced Electrochemical Performances of Metal Sulfides/Selenides for Sodium-Ion Capacitors: The Case of FeS _{2–<i>x</i>} Se _{<i>x</i>} . ACS Applied Materials & Interfaces, 2018, 10, 10945-10954. | 8.0 | 91 |
| 167 | Vacuum distillation derived 3D porous current collector for stable lithium–metal batteries. Nano Energy, 2018, 47, 503-511. | 16.0 | 221 |
| 168 | Heteroatom dopings and hierarchical pores of graphene for synergistic improvement of lithium–sulfur battery performance. Inorganic Chemistry Frontiers, 2018, 5, 1053-1061. | 6.0 | 22 |
| 169 | Few layer nitrogen-doped graphene with highly reversible potassium storage. Energy Storage Materials, 2018, 11, 38-46. | 18.0 | 206 |
| 170 | Conductive Nanocrystalline Niobium Carbide as Highâ€Efficiency Polysulfides Tamer for Lithiumâ€Sulfur Batteries. Advanced Functional Materials, 2018, 28, 1704865. | 14.9 | 210 |
| 171 | One step conversion of waste polyethylene to Cr ₃ C ₂ nanorods and Cr ₂ AlC particles under mild conditions. Inorganic Chemistry Frontiers, 2018, 5, 2893-2897. | 6.0 | 16 |
| 172 | Metallothermic Reduction of Molten Adduct [PCl4+][AlCl4–] at 50 °C to Amorphous Phosphorus or Crystallized Phosphides. ACS Applied Materials & Interfaces, 2018, 10, 42469-42474. | 8.0 | 5 |
| 173 | Layered-Structure SbPO ₄ /Reduced Graphene Oxide: An Advanced Anode Material for Sodium Ion Batteries. ACS Nano, 2018, 12, 12869-12878. | 14.6 | 87 |
| 174 | Micron-Sized Nanoporous Antimony with Tunable Porosity for High-Performance Potassium-Ion Batteries. ACS Nano, 2018, 12, 12932-12940. | 14.6 | 223 |
| 175 | Deciphering the Modulation Essence of p Bands in Co-Based Compounds on Li-S Chemistry. Joule, 2018, 2, 2681-2693. | 24.0 | 406 |
| 176 | Conductive and Polar Titanium Boride as a Sulfur Host for Advanced Lithium–Sulfur Batteries. Chemistry of Materials, 2018, 30, 6969-6977. | 6.7 | 101 |
| 177 | In Situ Li ₃ PS ₄ Solid‣tate Electrolyte Protection Layers for Superior Longâ€Life and Highâ€Rate Lithiumâ€Metal Anodes. Advanced Materials, 2018, 30, e1804684. | 21.0 | 140 |
| 178 | Metal-organic framework-derived Co0.85Se nanoparticles in N-doped carbon as a high-rate and long-lifespan anode material for potassium ion batteries. Materials Today Energy, 2018, 10, 241-248. | 4.7 | 107 |
| 179 | The Dualâ€Play of 3D Conductive Scaffold Embedded with Co, N Codoped Hollow Polyhedra toward Highâ€Performance Li–S Full Cell. Advanced Energy Materials, 2018, 8, 1802561. | 19.5 | 114 |
| 180 | Hierarchical Grapheneâ€Scaffolded Silicon/Graphite Composites as High Performance Anodes for Lithiumâ€Ion Batteries. Small, 2018, 14, e1802457. | 10.0 | 91 |

Υίται Qian

| # | Article | IF | CITATIONS |
|-----|--|------|-----------|
| 181 | Mechanical Pressing Route for Scalable Preparation of Microstructured/Nanostrutured Si/Graphite Composite for Lithium Ion Battery Anodes. ACS Sustainable Chemistry and Engineering, 2018, 6, 14230-14238. | 6.7 | 42 |
| 182 | Sandwich-like Ni2P nanoarray/nitrogen-doped graphene nanoarchitecture as a high-performance anode for sodium and lithium ion batteries. Data in Brief, 2018, 20, 1999-2002. | 1.0 | 11 |
| 183 | Crystal structural design of exposed planes: express channels, high-rate capability cathodes for lithium-ion batteries. Nanoscale, 2018, 10, 17435-17455. | 5.6 | 82 |
| 184 | Preparation of Sb nanoparticles in molten salt and their potassium storage performance and mechanism. Nanoscale, 2018, 10, 13236-13241. | 5.6 | 125 |
| 185 | A novel class of functional additives for cyclability enhancement of the sulfur cathode in lithium sulfur batteries. Inorganic Chemistry Frontiers, 2018, 5, 2013-2017. | 6.0 | 13 |
| 186 | Facile synthesis ofÂN,O-codoped hard carbon on the kilogram scale for fast capacitive sodium storage. Journal of Materials Chemistry A, 2018, 6, 16465-16474. | 10.3 | 50 |
| 187 | Molten-salt chemical exfoliation process for preparing two-dimensional mesoporous Si nanosheets as high-rate Li-storage anode. Nano Research, 2018, 11, 6294-6303. | 10.4 | 35 |
| 188 | Lithium phosphide/lithium chloride coating on lithium for advanced lithium metal anode. Journal of Materials Chemistry A, 2018, 6, 15859-15867. | 10.3 | 90 |
| 189 | Truncated cobalt hexacyanoferrate nanocubes threaded by carbon nanotubes as a high-capacity and high-rate cathode material for dual-ion rechargable aqueous batteries. Journal of Power Sources, 2018, 399, 1-7. | 7.8 | 35 |
| 190 | NiS _{1.03} Hollow Spheres and Cages as Superhigh Rate Capacity and Stable Anode Materials for Half/Full Sodium-Ion Batteries. ACS Nano, 2018, 12, 8277-8287. | 14.6 | 127 |
| 191 | Optimization of Microporous Carbon Structures for Lithium–Sulfur Battery Applications in Carbonateâ€Based Electrolyte. Small, 2017, 13, 1603533. | 10.0 | 64 |
| 192 | Facile synthesis and electrochemistry of a new cubic rocksalt Li _x V _y O ₂ (x = 0.78, y = 0.75) electrode material. Journal of Materials Chemistry A, 2017, 5, 5148-5155. | 10.3 | 7 |
| 193 | General Fabrication of Boride, Carbide, and Nitride Nanocrystals via a Metal-Hydrolysis-Assisted Process. Inorganic Chemistry, 2017, 56, 2440-2447. | 4.0 | 23 |
| 194 | Sulfurâ€Rich Phosphorus Sulfide Molecules for Use in Rechargeable Lithium Batteries. Angewandte Chemie - International Edition, 2017, 56, 2937-2941. | 13.8 | 50 |
| 195 | Simple synthesis of a porous Sb/Sb2O3 nanocomposite for a high-capacity anode material in Na-ion batteries. Nano Research, 2017, 10, 1794-1803. | 10.4 | 67 |
| 196 | Sulfurâ€Rich Phosphorus Sulfide Molecules for Use in Rechargeable Lithium Batteries. Angewandte Chemie, 2017, 129, 2983-2987. | 2.0 | 6 |
| 197 | MoSe ₂ â€Covered N,Pâ€Doped Carbon Nanosheets as a Longâ€Life and Highâ€Rate Anode Material for Sodiumâ€Ion Batteries. Advanced Functional Materials, 2017, 27, 1700522. | 14.9 | 454 |
| 198 | Surfactant widens the electrochemical window of an aqueous electrolyte for better rechargeable aqueous sodium/zinc battery. Journal of Materials Chemistry A, 2017, 5, 730-738. | 10.3 | 287 |

| # | Article | IF | CITATIONS |
|-----|---|------|-----------|
| 199 | Sb nanoparticles uniformly dispersed in 1-D N-doped porous carbon as anodes for Li-ion and Na-ion batteries. Journal of Materials Chemistry A, 2017, 5, 12144-12148. | 10.3 | 88 |
| 200 | Wetâ€Chemical Synthesis of Hollow Redâ€Phosphorus Nanospheres with Porous Shells as Anodes for Highâ€Performance Lithiumâ€ion and Sodiumâ€ion Batteries. Advanced Materials, 2017, 29, 1700214. | 21.0 | 213 |
| 201 | Ultramicroporous Carbon through an Activation-Free Approach for Li–S and Na–S Batteries in Carbonate-Based Electrolyte. ACS Applied Materials & Interfaces, 2017, 9, 13813-13818. | 8.0 | 61 |
| 202 | One-Dimensional Yolk–Shell Sb@Ti–O–P Nanostructures as a High-Capacity and High-Rate Anode Material for Sodium Ion Batteries. ACS Applied Materials & Interfaces, 2017, 9, 447-454. | 8.0 | 79 |
| 203 | One-step solid state reaction for the synthesis of ternary nitrides Co ₃ Mo ₃ N and Fe ₃ Mo ₃ N. Inorganic Chemistry Frontiers, 2017, 4, 2055-2058. | 6.0 | 8 |
| 204 | Controllable Self-Assembly of Micro-Nanostructured Si-Embedded Graphite/Graphene Composite Anode for High-Performance Li-Ion Batteries. ACS Applied Materials & Interfaces, 2017, 9, 39318-39325. | 8.0 | 64 |
| 205 | Scalable synthesis of carbon stabilized SiO/graphite sheets composite as anode for high-performance Li ion batteries. RSC Advances, 2017, 7, 39762-39766. | 3.6 | 22 |
| 206 | Biphase-Interface Enhanced Sodium Storage and Accelerated Charge Transfer: Flower-Like Anatase/Bronze TiO ₂ /C as an Advanced Anode Material for Na-Ion Batteries. ACS Applied Materials & Interfaces, 2017, 9, 43648-43656. | 8.0 | 63 |
| 207 | Sole Chemical Confinement of Polysulfides on Nonporous Nitrogen/Oxygen Dualâ€Doped Carbon at the Kilogram Scale for Lithium–Sulfur Batteries. Advanced Functional Materials, 2017, 27, 1604265. | 14.9 | 173 |
| 208 | Designed Formation of MnO ₂ @NiO/NiMoO ₄ Nanowires@Nanosheets Hierarchical Structures with Enhanced Pseudocapacitive Properties. ChemElectroChem, 2016, 3, 1347-1353. | 3.4 | 32 |
| 209 | Synthesis of MoS ₂ @C Nanotubes Via the Kirkendall Effect with Enhanced Electrochemical Performance for Lithium Ion and Sodium Ion Batteries. Small, 2016, 12, 2484-2491. | 10.0 | 192 |
| 210 | Hierarchical Carbon Nanotubes with a Thick Microporous Wall and Inner Channel as Efficient Scaffolds for Lithium–Sulfur Batteries. Advanced Functional Materials, 2016, 26, 1571-1579. | 14.9 | 177 |
| 211 | A Composite Structure of Cu ₃ Ge/Ge/C Anode Promise Better Rate Property for Lithium Battery. Small, 2016, 12, 6024-6032. | 10.0 | 26 |
| 212 | Synthesis of S/CoS2 Nanoparticles-Embedded N-doped Carbon Polyhedrons from Polyhedrons ZIF-67 and their Properties in Lithium-Sulfur Batteries. Electrochimica Acta, 2016, 218, 243-251. | 5.2 | 141 |
| 213 | B,N-Co-doped Graphene Supported Sulfur for Superior Stable Li–S Half Cell and Ge–S Full Battery. ACS Applied Materials & Interfaces, 2016, 8, 27679-27687. | 8.0 | 56 |
| 214 | MoO 2 nanoparticles as high capacity intercalation anode material for long-cycle lithium ion battery. Electrochimica Acta, 2016, 213, 416-422. | 5.2 | 26 |
| 215 | Direct Synthesis of Few-Layer F-Doped Graphene Foam and Its Lithium/Potassium Storage Properties. ACS Applied Materials & Interfaces, 2016, 8, 20682-20690. | 8.0 | 263 |
| 216 | A molten salt strategy for deriving a porous Si@C nano-composite from Si-rich biomass for high-performance Li-ion batteries. RSC Advances, 2016, 6, 79890-79893. | 3.6 | 12 |

Υίται Qian

| # | Article | IF | CITATIONS |
|-----|---|------|-----------|
| 217 | A simple melting-diffusing-reacting strategy to fabricate S/NiS ₂ –C for lithium–sulfur batteries. Nanoscale, 2016, 8, 17616-17622. | 5.6 | 100 |
| 218 | A scalable in situ surfactant-free synthesis of a uniform MnO/graphene composite for highly reversible lithium storage. Dalton Transactions, 2016, 45, 19221-19225. | 3.3 | 12 |
| 219 | One-pot hydrothermal synthesis of Nitrogen-doped graphene as high-performance anode materials for lithium ion batteries. Scientific Reports, 2016, 6, 26146. | 3.3 | 342 |
| 220 | Doubleâ€Walled Sb@TiO _{2â^'x} Nanotubes as a Superior Highâ€Rate and Ultralongâ€Lifespan Anode Material for Naâ€Ion and Liâ€Ion Batteries. Advanced Materials, 2016, 28, 4126-4133. | 21.0 | 412 |
| 221 | Design and synthesis of a stable-performance P2-type layered cathode material for sodium ion batteries. RSC Advances, 2016, 6, 55327-55330. | 3.6 | 6 |
| 222 | One-step thermolysis synthesis of two-dimensional ultrafine Fe ₃ O ₄ particles/carbon nanonetworks for high-performance lithium-ion batteries. Nanoscale, 2016, 8, 4733-4741. | 5.6 | 67 |
| 223 | A Deep Reduction and Partial Oxidation Strategy for Fabrication of Mesoporous Si Anode for Lithium Ion Batteries. ACS Nano, 2016, 10, 2295-2304. | 14.6 | 121 |
| 224 | Trace Fe ³⁺ mediated synthesis of LiFePO ₄ micro/nanostructures towards improved electrochemical performance for lithium-ion batteries. RSC Advances, 2016, 6, 456-463. | 3.6 | 17 |
| 225 | Porous silicon nano-aggregate from silica fume as an anode for high-energy lithium-ion batteries. RSC Advances, 2016, 6, 30577-30581. | 3.6 | 15 |
| 226 | A graphene oxide-wrapped bipyramidal sulfur@polyaniline core–shell structure as a cathode for Li–S batteries with enhanced electrochemical performance. Journal of Materials Chemistry A, 2016, 4, 6404-6410. | 10.3 | 98 |
| 227 | A scalable synthesis of N-doped Si nanoparticles for high-performance Li-ion batteries. Chemical Communications, 2016, 52, 3813-3816. | 4.1 | 26 |
| 228 | In situ growth of carbon nanotube wrapped Si composites as anodes for high performance lithium ion batteries. Nanoscale, 2016, 8, 4903-4907. | 5.6 | 30 |
| 229 | Origin of additional capacities in selenium-based ZnSe@C nanocomposite Li-ion battery electrodes. Electrochemistry Communications, 2016, 65, 44-47. | 4.7 | 49 |
| 230 | Mesh-like LiZnBO ₃ /C composites as a prominent stable anode for lithium ion rechargeable batteries. Journal of Materials Chemistry A, 2016, 4, 5489-5494. | 10.3 | 13 |
| 231 | Na-birnessite with high capacity and long cycle life for rechargeable aqueous sodium-ion battery cathode electrodes. Journal of Materials Chemistry A, 2016, 4, 856-860. | 10.3 | 62 |
| 232 | Hydrothermal Synthesis of Unique Hollow Hexagonal Prismatic Pencils of Co ₃ V ₂ O ₈ â‹ <i>n</i> H ₂ O: A New Anode Material for Lithiumâ€Ion Batteries. Angewandte Chemie - International Edition, 2015, 54, 10787-10791. | 13.8 | 115 |
| 233 | A Facile Method for Synthesis of Porous NiCo ₂ O ₄ Nanorods as a High-Performance Anode Material for Li-Ion Batteries. Particle and Particle Systems Characterization, 2015, 32, 1012-1019. | 2.3 | 63 |
| 234 | One-Pot Hydrothermal Synthesis of FeMoO ₄ Nanocubes as an Anode Material for Lithium-Ion Batteries with Excellent Electrochemical Performance. Small, 2015, 11, 4753-4761. | 10.0 | 87 |

| # | Article | IF | CITATIONS |
|-----|---|------|-----------|
| 235 | A New Saltâ€Baked Approach for Confining Selenium in Metal Complexâ€Derived Porous Carbon with Superior Lithium Storage Properties. Advanced Functional Materials, 2015, 25, 5229-5238. | 14.9 | 117 |
| 236 | Porous MnFe ₂ O ₄ microrods as advanced anodes for Li-ion batteries with long cycle lifespan. Journal of Materials Chemistry A, 2015, 3, 9550-9555. | 10.3 | 49 |
| 237 | Rational design of SnO2 aggregation nanostructure with uniform pores and its supercapacitor application. Journal of Materials Science: Materials in Electronics, 2015, 26, 6143-6147. | 2.2 | 10 |
| 238 | Polyaniline-Assisted Synthesis of Si@C/RGO as Anode Material for Rechargeable Lithium-Ion Batteries. ACS Applied Materials & Interfaces, 2015, 7, 409-414. | 8.0 | 78 |
| 239 | Coaxial MnO/N-doped carbon nanorods for advanced lithium-ion battery anodes. Journal of Materials Chemistry A, 2015, 3, 1037-1041. | 10.3 | 192 |
| 240 | A synchronous approach for facile production of Ge–carbon hybrid nanoparticles for high-performance lithium batteries. Chemical Communications, 2015, 51, 3882-3885. | 4.1 | 40 |
| 241 | Preparation of Nanocrystalline Silicon from SiCl ₄ at 200 °C in Molten Salt for Highâ€Performance Anodes for Lithium Ion Batteries. Angewandte Chemie - International Edition, 2015, 54, 3822-3825. | 13.8 | 154 |
| 242 | Electrochemical performance of rod-like Sb–C composite as anodes for Li-ion and Na-ion batteries. Journal of Materials Chemistry A, 2015, 3, 3276-3280. | 10.3 | 94 |
| 243 | High yield fabrication of hollow vesica-like silicon based on the Kirkendall effect and its application to energy storage. Nanoscale, 2015, 7, 3440-3444. | 5.6 | 51 |
| 244 | A potential pyrrhotite (Fe ₇ S ₈) anode material for lithium storage. RSC Advances, 2015, 5, 14828-14831. | 3.6 | 65 |
| 245 | The design of a high-energy Li-ion battery using germanium-based anode and LiCoO2 cathode. Journal of Power Sources, 2015, 293, 868-875. | 7.8 | 47 |
| 246 | Facile fabrication of hierarchical porous rose-like NiCo ₂ O ₄ nanoflake/MnCo ₂ O ₄ nanoparticle composites with enhanced electrochemical performance for energy storage. Journal of Materials Chemistry A, 2015, 3, 16142-16149. | 10.3 | 106 |
| 247 | Synchronous synthesis of a Si/Cu/C ternary nano-composite as an anode for Li ion batteries. Journal of Materials Chemistry A, 2015, 3, 17544-17548. | 10.3 | 13 |
| 248 | Amorphous S-rich S _{1â^'x} Se _x /C (x ≤0.1) composites promise better lithium–sulfur batteries in a carbonate-based electrolyte. Energy and Environmental Science, 2015, 8, 3181-3186. | 30.8 | 164 |
| 249 | Rationally designed hierarchical MnO ₂ @NiO nanostructures for improved lithium ion storage. RSC Advances, 2015, 5, 61148-61154. | 3.6 | 9 |
| 250 | Enhancing the electrode performance of Co ₃ O ₄ through Co ₃ O ₄ @a-TiO ₂ core–shell microcubes with controllable pore size. RSC Advances, 2015, 5, 40899-40906. | 3.6 | 7 |
| 251 | Hydrogenated TiO ₂ Branches Coated Mn ₃ O ₄ Nanorods as an Advanced Anode Material for Lithium Ion Batteries. ACS Applied Materials & Interfaces, 2015, 7, 10348-10355. | 8.0 | 81 |
| 252 | Mnâ€Doped αâ€FeOOH Nanorods and αâ€Fe ₂ O ₃ Mesoporous Nanorods: Facile Synthesis and Applications as High Performance Anodes for LIBs. Advanced Electronic Materials, 2015, 1, 1400057. | 5.1 | 55 |

| # | Article | IF | CITATIONS |
|-----|--|------|-----------|
| 253 | Honeycomb-like Macro-Germanium as High-Capacity Anodes for Lithium-Ion Batteries with Good Cycling and Rate Performance. Chemistry of Materials, 2015, 27, 4156-4164. | 6.7 | 70 |
| 254 | Mn ₃ O ₄ @C core–shell composites as an improved anode for advanced lithium ion batteries. RSC Advances, 2015, 5, 46829-46833. | 3.6 | 14 |
| 255 | A Si/Ge nanocomposite prepared by a one-step solid-state metathesis reaction and its enhanced electrochemical performance. Journal of Materials Chemistry A, 2015, 3, 11199-11202. | 10.3 | 26 |
| 256 | Nanoporous germanium as high-capacity lithium-ion battery anode. Nano Energy, 2015, 13, 651-657. | 16.0 | 131 |
| 257 | Mesoporous quasi-single-crystalline NiCo ₂ O ₄ superlattice nanoribbons with optimizable lithium storage properties. Journal of Materials Chemistry A, 2015, 3, 10336-10344. | 10.3 | 78 |
| 258 | Chemical synthesis of porous hierarchical Ge–Sn binary composites using metathesis reaction for rechargeable Li-ion batteries. Chemical Communications, 2015, 51, 17156-17159. | 4.1 | 27 |
| 259 | A low temperature molten salt process for aluminothermic reduction of silicon oxides to crystalline Si for Li-ion batteries. Energy and Environmental Science, 2015, 8, 3187-3191. | 30.8 | 193 |
| 260 | Triple-walled SnO ₂ @N-doped carbon@SnO ₂ nanotubes as an advanced anode material for lithium and sodium storage. Journal of Materials Chemistry A, 2015, 3, 23194-23200. | 10.3 | 68 |
| 261 | Synchronously synthesized Si@C composites through solvothermal oxidation of Mg ₂ Si as lithium ion battery anode. RSC Advances, 2015, 5, 71355-71359. | 3.6 | 8 |
| 262 | Silicon nanoparticles obtained via a low temperature chemical "metathesis―synthesis route and their lithium-ion battery properties. Chemical Communications, 2015, 51, 2345-2348. | 4.1 | 53 |
| 263 | An aqueous rechargeable sodium ion battery based on a NaMnO ₂ –NaTi ₂ (PO ₄) ₃ hybrid system for stationary energy storage. Journal of Materials Chemistry A, 2015, 3, 1400-1404. | 10.3 | 179 |
| 264 | Hydrothermal synthesis of nano-silicon from a silica sol and its use in lithium ion batteries. Nano Research, 2015, 8, 1497-1504. | 10.4 | 62 |
| 265 | Anodes: Unusual Formation of ZnCo2O43D Hierarchical Twin Microspheres as a High-Rate and Ultralong-Life Lithium-Ion Battery Anode Material (Adv. Funct. Mater. 20/2014). Advanced Functional Materials, 2014, 24, 3011-3011. | 14.9 | 2 |
| 266 | Comparison between SnSb–C and Sn–C composites as anode materials for lithium-ion batteries. RSC Advances, 2014, 4, 62301-62307. | 3.6 | 23 |
| 267 | A comparative study of lithium-storage performances of hematite: Nanotubes vs. nanorods. Journal of Power Sources, 2014, 245, 429-435. | 7.8 | 62 |
| 268 | Unusual Formation of ZnCo ₂ O ₄ 3D Hierarchical Twin Microspheres as a Highâ€Rate and Ultralongâ€Life Lithiumâ€Ion Battery Anode Material. Advanced Functional Materials, 2014, 24, 3012-3020. | 14.9 | 382 |
| 269 | Stable Cycling of Fe ₂ O ₃ Nanorice as an Anode through Electrochemical Porousness and the Solid–Electrolyte Interphase Thermolysis Approach. ChemPlusChem, 2014, 79, 143-150. | 2.8 | 14 |
| 270 | Hierarchical core–shell α-Fe2O3@C nanotubes as a high-rate and long-life anode for advanced lithium ion batteries. Journal of Materials Chemistry A, 2014, 2, 3439-3444. | 10.3 | 55 |

| # | Article | IF | CITATIONS |
|-----|--|------|-----------|
| 271 | Fabrication of one-dimensional SnO2/MoO3/C nanostructure assembled of stacking SnO2 nanosheets from its heterostructure precursor and its application in lithium-ion batteries. Journal of Materials Chemistry A, 2014, 2, 9784. | 10.3 | 38 |
| 272 | Recycling chicken eggshell membranes for high-capacity sodium battery anodes. RSC Advances, 2014, 4, 50950-50954. | 3.6 | 31 |
| 273 | Synthesis of novel morphologies of Li2FeSiO4/C micro/nano composites by a facile hydrothermal method. RSC Advances, 2014, 4, 39889-39893. | 3.6 | 9 |
| 274 | Embedding silicon nanoparticles in graphene based 3D framework by cross-linking reaction for high performance lithium ion batteries. Journal of Materials Chemistry A, 2014, 2, 19604-19608. | 10.3 | 39 |
| 275 | From ultrathin nanosheets, triangular plates to nanocrystals with exposed (102) facets, a morphology and phase transformation of sp2 hybrid BN nanomaterials. RSC Advances, 2014, 4, 14233. | 3.6 | 26 |
| 276 | One-pot synthesis of carbon nanoribbons and their enhanced lithium storage performance. Journal of Materials Chemistry A, 2014, 2, 11974-11979. | 10.3 | 14 |
| 277 | A facile synthesis of highly porous CdSnO3 nanoparticles and their enhanced performance in lithium-ion batteries. Journal of Materials Chemistry A, 2014, 2, 4970. | 10.3 | 10 |
| 278 | Bulk Ti ₂ Nb ₁₀ O ₂₉ as long-life and high-power Li-ion battery anodes. Journal of Materials Chemistry A, 2014, 2, 17258-17262. | 10.3 | 112 |
| 279 | Synthesis of Co2SnO4 hollow cubes encapsulated in graphene as high capacity anode materials for lithium-ion batteries. Journal of Materials Chemistry A, 2014, 2, 2728. | 10.3 | 68 |
| 280 | Facile synthesis of hierarchically porous NiO micro-tubes as advanced anode materials for lithium-ion batteries. Journal of Materials Chemistry A, 2014, 2, 16847-16850. | 10.3 | 73 |
| 281 | General synthesis of hollow MnO ₂ , Mn ₃ O ₄ and MnO nanospheres as superior anode materials for lithium ion batteries. Journal of Materials Chemistry A, 2014, 2, 17421-17426. | 10.3 | 213 |
| 282 | Synthesis of urchin-like Sn–ZnO–C composite and its enhanced electrochemical performance for lithium-ion batteries. Science Bulletin, 2014, 59, 2006-2011. | 1.7 | 4 |
| 283 | Layer structured α-FeSe: A potential anode material for lithium storage. Electrochemistry Communications, 2014, 38, 124-127. | 4.7 | 62 |
| 284 | Graphene-Supported NaTi ₂ (PO ₄) ₃ as a High Rate Anode Material for Aqueous Sodium Ion Batteries. Journal of the Electrochemical Society, 2014, 161, A1181-A1187. | 2.9 | 98 |
| 285 | 3D Co ₃ O ₄ and CoO@C wall arrays: morphology control, formation mechanism, and lithium-storage properties. Journal of Materials Chemistry A, 2014, 2, 11597. | 10.3 | 81 |
| 286 | One pot synthesis of ultrathin boron nitride nanosheet-supported nanoscale zerovalent iron for rapid debromination of polybrominated diphenyl ethers. Journal of Materials Chemistry A, 2013, 1, 6379. | 10.3 | 52 |
| 287 | Facile synthesis of mesoporous Mn3O4 nanotubes and their excellent performance for lithium-ion batteries. Journal of Materials Chemistry A, 2013, 1, 10985. | 10.3 | 114 |
| 288 | Simple synthesis of yolk-shelled ZnCo2O4 microspheres towards enhancing the electrochemical performance of lithium-ion batteries in conjunction with a sodium carboxymethyl cellulose binder. Journal of Materials Chemistry A, 2013, 1, 15292. | 10.3 | 151 |

| # | Article | IF | CITATIONS |
|-----|---|------|-----------|
| 289 | Formation of Grapheneâ€Wrapped Nanocrystals at Room Temperature through the Colloidal Coagulation Effect. Particle and Particle Systems Characterization, 2013, 30, 143-147. | 2.3 | 39 |
| 290 | Controlled Growth of Porous αâ€Fe ₂ O ₃ Branches on βâ€MnO ₂ Nanorods for Excellent Performance in Lithiumâ€Ion Batteries. Advanced Functional Materials, 2013, 23, 4049-4056. | 14.9 | 181 |
| 291 | Effect of different carbon sources on the electrochemical properties of rod-like LiMnPO4–C nanocomposites. RSC Advances, 2013, 3, 6847. | 3.6 | 37 |
| 292 | MnO@1-D carbon composites from the precursor C4H4MnO6 and their high-performance in lithium batteries. RSC Advances, 2013, 3, 10001. | 3.6 | 69 |
| 293 | Spinel Mn1.5Co1.5O4 core–shell microspheres as Li-ion battery anode materials with a long cycle life and high capacity. Journal of Materials Chemistry, 2012, 22, 23254. | 6.7 | 140 |
| 294 | A new carbon intercalated compound of Dion–Jacobson phase HLaNb2O7. Journal of Materials Chemistry, 2012, 22, 11086. | 6.7 | 35 |
| 295 | Synthesis of MnO@C core–shell nanoplates with controllable shell thickness and their electrochemical performance for lithium-ion batteries. Journal of Materials Chemistry, 2012, 22, 17864. | 6.7 | 114 |
| 296 | Synthesis of TiN hollow sphere by a modified one-step template self-assembly method. CrystEngComm, 2012, 14, 2186. | 2.6 | 5 |
| 297 | Facile synthesis of uniform h-BN nanocrystals and their application as a catalyst support towards the selective oxidation of benzyl alcohol. RSC Advances, 2012, 2, 10689. | 3.6 | 20 |
| 298 | A facile room-temperature route to flower-like CuO microspheres with greatly enhanced lithium storage capability. RSC Advances, 2012, 2, 8602. | 3.6 | 40 |
| 299 | Solid state synthesis of a new ternary nitride MgMoN2 nanosheets and micromeshes. Journal of Materials Chemistry, 2012, 22, 14559. | 6.7 | 25 |
| 300 | A novel benzene–water azeotrope route to new Na-based metal fluorosulphates NaFeSO4F and NaFeSO4F·2H2O in one minute. CrystEngComm, 2012, 14, 4251. | 2.6 | 11 |
| 301 | Synthesis, characterization and application of carbon nanocages as anode materials for high-performance lithium-ion batteries. RSC Advances, 2012, 2, 284-291. | 3.6 | 62 |
| 302 | Mesoporous NiO ultrathin nanowire networks topotactically transformed from α-Ni(OH)2 hierarchical microspheres and their superior electrochemical capacitance properties and excellent capability for water treatment. Journal of Materials Chemistry, 2012, 22, 14276. | 6.7 | 139 |
| 303 | Hydrothermal synthesis of layered Li1.81H0.19Ti2O5·xH2O nanosheets and their transformation to single-crystalline Li4Ti5O12 nanosheets as the anode materials for Li-ion batteries. CrystEngComm, 2012, 14, 6435. | 2.6 | 47 |
| 304 | Fabrication of single-crystalline CuInS2 nanowires array via a diethylenetriamine-thermal route. CrystEngComm, 2012, 14, 7217. | 2.6 | 22 |
| 305 | A thermal reduction route to nanocrystalline transition metal carbides from waste polytetrafluoroethylene and metal oxides. Materials Chemistry and Physics, 2012, 137, 1-4. | 4.0 | 24 |
| 306 | Synthesis of Mn ₃ O ₄ nanowires and their transformation to LiMn ₂ O ₄ polyhedrons, application of LiMn ₂ O ₄ as a cathode in a lithium-ion battery. CrystEngComm, 2012, 14, 1485-1489. | 2.6 | 30 |

| # | Article | IF | CITATIONS |
|-----|---|------|-----------|
| 307 | Synchronously synthesized core–shell LiNi1/3Co1/3Mn1/3O2/carbon nanocomposites as cathode materials for high performance lithium ion batteries. RSC Advances, 2012, 2, 12886. | 3.6 | 38 |
| 308 | Facile synthesis of nanocrystalline-assembled bundle-like CuO nanostructure with high rate capacities and enhanced cycling stability as an anode material for lithium-ion batteries. Journal of Materials Chemistry, 2012, 22, 11297. | 6.7 | 66 |
| 309 | Enhanced energy storage and rate performance induced by dense nanocavities inside MnWO4 nanobars. RSC Advances, 2012, 2, 6748. | 3.6 | 30 |
| 310 | Synthesis of superconducting sphereâ€like Mo ₂ C nanoparticles in an autoclave. Crystal Research and Technology, 2012, 47, 467-470. | 1.3 | 5 |
| 311 | One-step hydrothermal synthesis of ZnFe2O4 nano-octahedrons as a high capacity anode material for Li-ion batteries. Nano Research, 2012, 5, 477-485. | 10.4 | 241 |
| 312 | Magnesium-assisted formation of metal carbides and nitrides from metal oxides. International Journal of Refractory Metals and Hard Materials, 2012, 31, 288-292. | 3.8 | 23 |
| 313 | Preparation of LiCoO2 concaved cuboctahedra and their electrochemical behavior in lithium-ion battery. Dalton Transactions, 2011, 40, 7645. | 3.3 | 27 |
| 314 | Mesoporous NiO with various hierarchical nanostructures by quasi-nanotubes/nanowires/nanorodsself-assembly: controllable preparation and application in supercapacitors. CrystEngComm, 2011, 13, 626-632. | 2.6 | 121 |
| 315 | Fabrication of $\hat{1}^3$ -MnO2/ $\hat{1}\pm$ -MnO2 hollow core/shell structures and their application to water treatment. Journal of Materials Chemistry, 2011, 21, 16210. | 6.7 | 94 |
| 316 | Convenient synthesis and applications of gram scale boron nitride nanosheets. Catalysis Science and Technology, 2011, 1, 1119. | 4.1 | 53 |
| 317 | Solid state synthesis of nitride, carbide and boride nanocrystals in an autoclave. Journal of Materials Chemistry, 2011, 21, 13756. | 6.7 | 22 |
| 318 | Formation and morphology control of nanoparticles via solution routes in an autoclave. Journal of Materials Chemistry, 2011, 21, 11457. | 6.7 | 93 |
| 319 | Cadmium sulfide rod-bundle structures decorated with nanoparticles from an inorganic/organic composite. Journal of Nanoparticle Research, 2011, 13, 3535-3543. | 1.9 | 4 |
| 320 | Synthesis and magnetic properties of Fe3O4/helical carbon nanofiber nanocomposites from the catalytic pyrolysis of ferrocene. Science Bulletin, 2011, 56, 3199. | 1.7 | 3 |
| 321 | Synthesis, transformation to octahedronâ€like crystals, and gasâ€sensing property of sixâ€horned nanospheres of Cu ₂ 0. Crystal Research and Technology, 2011, 46, 967-972. | 1.3 | 0 |
| 322 | Carbide Nanoparticles Encapsulated in the Caves of Carbon Nanotubes by an In Situ Reduction-Carbonization Route. Journal of Nanomaterials, 2011, 2011, 1-5. | 2.7 | 32 |
| 323 | Malic acid assisted precursor route to hierarchical structured nickel oxide. Crystal Research and Technology, 2010, 45, 545-550. | 1.3 | 5 |
| 324 | Mgâ€Assisted Autoclave Synthesis of RB ₆ (R = Sm, Eu, Gd, and Tb) Submicron Cubes and SmB ₆ Submicron Rods. European Journal of Inorganic Chemistry, 2010, 2010, 1289-1294. | 2.0 | 26 |

| # | Article | IF | CITATIONS |
|-----|---|------|-----------|
| 325 | Double‧helled Mn ₂ O ₃ Hollow Spheres and Their Application in Water Treatment. European Journal of Inorganic Chemistry, 2010, 2010, 1172-1176. | 2.0 | 42 |
| 326 | Synthesis and Electrical Capacitance of Carbon Nanoplates. European Journal of Inorganic Chemistry, 2010, 2010, 4314-4320. | 2.0 | 12 |
| 327 | A simple pyrolysis route to synthesize leaf-like carbon sheets. Carbon, 2010, 48, 3420-3426. | 10.3 | 20 |
| 328 | Orthogonal Designâ€Assisted Solvothermal Strategy for Preparing Silicon Nitride Nanodendrites on a Large Scale. International Journal of Applied Ceramic Technology, 2010, 7, 889-894. | 2.1 | 3 |
| 329 | Hydrothermal Synthesis and Electrochemical Properties of Urchin-Like Coreâ^'Shell Copper Oxide Nanostructures. Journal of Physical Chemistry C, 2010, 114, 9645-9650. | 3.1 | 66 |
| 330 | CdS Hierarchical Nanostructures with Tunable Morphologies: Preparation and Photocatalytic Properties. Journal of Physical Chemistry C, 2010, 114, 14029-14035. | 3.1 | 117 |
| 331 | Recent Development of the Synthesis and Engineering Applications of One-Dimensional Boron Nitride Nanomaterials. Journal of Nanomaterials, 2010, 2010, 1-16. | 2.7 | 12 |
| 332 | A versatile route for the convenient synthesis of rare-earth and alkaline-earth hexaborides at mild temperatures. CrystEngComm, 2010, 12, 3923. | 2.6 | 43 |
| 333 | Tartatric Acid and <scp>L</scp> ysteine Synergisticâ€Assisted Synthesis of Antimony Trisulfide Hierarchical Structures in Aqueous Solution. European Journal of Inorganic Chemistry, 2009, 2009, 5302-5306. | 2.0 | 15 |
| 334 | Solution-phase synthesis of nanomaterials at low temperature. Science in China Series G: Physics, Mechanics and Astronomy, 2009, 52, 13-20. | 0.2 | 14 |
| 335 | Additiveâ€Assisted Nitridation to Synthesize Si ₃ N ₄ Nanomaterials at a Low Temperature. Journal of the American Ceramic Society, 2009, 92, 517-519. | 3.8 | 12 |
| 336 | The synthesis of nanostructured SiC from waste plastics and silicon powder. Nanotechnology, 2009, 20, 355604. | 2.6 | 29 |
| 337 | Acetylacetone-Directed Controllable Synthesis of Bi2S3 Nanostructures with Tunable Morphology. Crystal Growth and Design, 2009, 9, 3862-3867. | 3.0 | 61 |
| 338 | Sunlight-assisted fabrication of a hierarchical ZnO nanorod array structure. CrystEngComm, 2009, 11, 2009. | 2.6 | 26 |
| 339 | Thermal-induced shape evolution from uniform triangular to hexagonal r-BN nanoplates. Journal of Materials Chemistry, 2009, 19, 8086. | 6.7 | 30 |
| 340 | Growth and characterization of ZnS porous nanoribbon array constructed by connected nanocrystallities. CrystEngComm, 2009, 11, 2308. | 2.6 | 15 |
| 341 | A general route for the convenient synthesis of crystalline hexagonal boron nitride micromesh at mild temperature. Journal of Materials Chemistry, 2009, 19, 1989. | 6.7 | 51 |
| 342 | Largeâ€Scale Synthesis of Magnenium Silicon Nitride Powders at Low Temperature. Journal of the American Ceramic Society, 2008, 91, 333-336. | 3.8 | 11 |

| # | Article | IF | CITATIONS |
|-----|--|-----|-----------|
| 343 | Synthesis of MnV2O6 nanoflakes via simple hydrothermal process. Frontiers of Chemistry in China: Selected Publications From Chinese Universities, 2008, 3, 275-278. | 0.4 | 6 |
| 344 | Sulfurâ€Assisted Approach for the Lowâ€Temperature Synthesis of β‣iC Nanowires. European Journal of Inorganic Chemistry, 2008, 2008, 3883-3888. | 2.0 | 30 |
| 345 | Solvothermal Synthesis of Si ₃ N ₄ Nanomaterials at a Low Temperature. Journal of the American Ceramic Society, 2008, 91, 1725-1728. | 3.8 | 21 |
| 346 | Controlled fabrication of SnO2 solid and hollow nanocubes with a simple hydrothermal route. Applied Physics Letters, 2008, 93, 152511. | 3.3 | 26 |
| 347 | A Facile Approach for the Synthesis of Uniform Hollow Carbon Nanospheres. Journal of Physical Chemistry C, 2008, 112, 1896-1900. | 3.1 | 29 |
| 348 | Hydrothermal Growth and Morphology Modification of β-NiS Three-Dimensional Flowerlike Architectures. Crystal Growth and Design, 2007, 7, 1918-1922. | 3.0 | 99 |
| 349 | Shape-Controlled Synthesis of Tellurium 1D Nanostructures via a Novel Circular Transformation Mechanism. Crystal Growth and Design, 2007, 7, 1185-1191. | 3.0 | 40 |
| 350 | Solution-Phase Synthesis of Single-Crystal CuO Nanoribbons and Nanorings. Crystal Growth and Design, 2007, 7, 930-934. | 3.0 | 150 |
| 351 | Synthesis of Kelp-Like Crystalline ?-SiC Nanobelts and their Apical Growth Mechanism. Journal of the American Ceramic Society, 2007, 90, 653-656. | 3.8 | 14 |
| 352 | <scp>l</scp> -Cysteine-Assisted Tunable Synthesis of PbS of Various Morphologies. Journal of Physical Chemistry C, 2007, 111, 16761-16767. | 3.1 | 96 |
| 353 | High-Yield Synthesis of NiO Nanoplatelets and Their Excellent Electrochemical Performance. Crystal Growth and Design, 2006, 6, 2163-2165. | 3.0 | 132 |
| 354 | lsostructural Cd3E2(E = P, As) Microcrystals Prepared via a Hydrothermal Route. Crystal Growth and Design, 2006, 6, 849-853. | 3.0 | 18 |
| 355 | Double-Source Approach to In2S3 Single Crystallites and Their Electrochemical Properties. Crystal Growth and Design, 2006, 6, 1304-1307. | 3.0 | 69 |
| 356 | The Fabrication and Characterization of Single-Crystalline Selenium Nanoneedles. Crystal Growth and Design, 2006, 6, 1711-1716. | 3.0 | 36 |
| 357 | Large-Scale Synthesis and Growth Mechanism of Single-Crystal Se Nanobelts. Crystal Growth and Design, 2006, 6, 1514-1517. | 3.0 | 51 |
| 358 | A Chemical Co-Reduction Route to Synthesize Nanocrystalline Vanadium Carbide. Journal of the American Ceramic Society, 2006, 89, 320-322. | 3.8 | 12 |
| 359 | Preparation of Semiconductor/Polymer Coaxial Nanocables by a Facile Solution Process. European Journal of Inorganic Chemistry, 2006, 2006, 207-212. | 2.0 | 8 |
| 360 | A Hydrothermal Reduction Route to Single-Crystalline Hexagonal Cobalt Nanowires. European Journal of Inorganic Chemistry, 2006, 2006, 2454-2459. | 2.0 | 110 |

| # | Article | IF | CITATIONS |
|-----|---|-----|-----------|
| 361 | Synthesis of Nanocrystalline Boron Carbide via a Solvothermal Reduction of CCl ₄ in the Presence of Amorphous Boron Powder. Journal of the American Ceramic Society, 2005, 88, 225-227. | 3.8 | 31 |
| 362 | Shape-Induced Enhanced Luminescent Properties of Red Phosphors: Sr2MgSi2O7:Eu3+ Nanotubes. European Journal of Inorganic Chemistry, 2005, 2005, 4031-4034. | 2.0 | 15 |
| 363 | Synthesis, Characterization, and Growth Mechanism of Tellurium Nanotubes. Crystal Growth and Design, 2005, 5, 325-328. | 3.0 | 137 |
| 364 | InP nanocrystals via surfactant-aided hydrothermal synthesis. Journal of Applied Physics, 2004, 95, 3683-3688. | 2.5 | 34 |
| 365 | Polyol-mediated preparation of disklike (ZnSe)2·EN precursor and its conversion to ZnSe crystals with quasi-network structure. Journal of Materials Research, 2004, 19, 1369-1373. | 2.6 | 6 |
| 366 | Lowâ€Temperature Synthesis of Nanocrystalline αâ€5i ₃ N ₄ Powders by the Reaction of Mg ₂ Si with NH ₄ Cl. Journal of the American Ceramic Society, 2004, 87, 1810-1813. | 3.8 | 12 |
| 367 | One-Dimensional Arrays of Co3O4Nanoparticles:Â Synthesis, Characterization, and Optical and Electrochemical Properties. Journal of Physical Chemistry B, 2004, 108, 16401-16404. | 2.6 | 249 |
| 368 | A Rational Self-Sacrificing Template Route toβ-Bi2O3 Nanotube Arrays. European Journal of Inorganic Chemistry, 2004, 2004, 1785-1787. | 2.0 | 85 |
| 369 | Selected-Control Solvothermal Synthesis of Nanoscale Hollow Spheres and Single-Crystal Tubes of PbTe. European Journal of Inorganic Chemistry, 2004, 2004, 4521-4524. | 2.0 | 55 |
| 370 | Formation of Carbon Nanotubes and Cubic and Spherical Nanocages. Journal of Physical Chemistry B, 2004, 108, 20090-20094. | 2.6 | 21 |
| 371 | Lithium-Assisted Synthesis and Characterization of Crystalline 3Câ^'SiC Nanobelts. Journal of Physical Chemistry B, 2004, 108, 20102-20104. | 2.6 | 130 |
| 372 | CuBr Crystal Growth in Ethylene Glycol Solvent by the Temperature-Difference Method. Crystal Growth and Design, 2004, 4, 413-414. | 3.0 | 18 |
| 373 | Single-step synthesis of copper sulfide hollow spheres by a template interface reaction routeElectronic supplementary information (ESI) available: XRD pattern of copper sulfide products. See http://www.rsc.org/suppdata/jm/b4/b407435a/. Journal of Materials Chemistry, 2004, 14, 2489. | 6.7 | 66 |
| 374 | Synthesis of nanocrystalline MoN from a new precursor by TPR method. Journal of Materials Science, 2003, 38, 3473-3478. | 3.7 | 12 |
| 375 | Solvothermal synthesis of titanium phosphides via sodium co-reduction of PCl3 and TiCl4. Journal of Materials Science Letters, 2003, 22, 1463-1464. | 0.5 | 3 |
| 376 | Large-Scale Synthesis of High Quality Trigonal Selenium Nanowires. European Journal of Inorganic Chemistry, 2003, 2003, 3250-3255. | 2.0 | 61 |
| 377 | A Template-Interface Co-Reduction Synthesis of Hollow Sphere-like Carbides. European Journal of Inorganic Chemistry, 2003, 2003, 3534-3537. | 2.0 | 13 |
| 378 | A Room-Temperature Route to Bismuth Nanotube Arrays. European Journal of Inorganic Chemistry, 2003, 2003, 3699-3702. | 2.0 | 47 |

| # | Article | IF | CITATIONS |
|-----|--|-----|-----------|
| 379 | A Complex-Based Soft Template Route to PbSe Nanowires. European Journal of Inorganic Chemistry, 2003, 2003, 644-647. | 2.0 | 29 |
| 380 | Reductionâ€Nitridation Synthesis of Titanium Nitride Nanocrystals. Journal of the American Ceramic Society, 2003, 86, 206-208. | 3.8 | 42 |
| 381 | Selective synthesis and characterization of famatinite nanofibers and tetrahedrite nanoflakes. Journal of Materials Chemistry, 2003, 13, 301-303. | 6.7 | 56 |
| 382 | A Co-pyrolysis Method to Boron Nitride Nanotubes at Relative Low Temperature. Chemistry of Materials, 2003, 15, 2675-2680. | 6.7 | 68 |
| 383 | Soft solution processing of cerium hydroxysulfate powders with different morphologies. Journal of Materials Chemistry, 2003, 13, 150-153. | 6.7 | 21 |
| 384 | Surfactant-assisted growth of uniform nanorods of crystalline tellurium. Journal of Materials Chemistry, 2003, 13, 159-162. | 6.7 | 97 |
| 385 | Low-temperature route to nanoscale P ₃ N ₅ hollow spheres. Journal of Materials Research, 2003, 18, 2359-2363. | 2.6 | 34 |
| 386 | Wet Synthesis and Characterization of MSe (M = Cd, Hg) Nanocrystallites at Room Temperature. Journal of Materials Research, 2002, 17, 1147-1152. | 2.6 | 16 |
| 387 | Fabrication of BiTel submicrometer hollow spheresElectronic supplementary information (ESI) available: XRD pattern and TEM images of Bi2Te3. See http://www.rsc.org/suppdata/jm/b2/b200950c/. Journal of Materials Chemistry, 2002, 12, 2426-2429. | 6.7 | 38 |
| 388 | Synthesis of closed PbS nanowires with regular geometric morphologiesElectronic supplementary information (ESI) available: XRD pattern of the PbS CNWs, FTIR spectrum of the polymer, TEM images of more PbS CNWs. See http://www.rsc.org/suppdata/jm/b1/b111187f/. Journal of Materials Chemistry, 2002, 12, 403-405. | 6.7 | 205 |
| 389 | Microwave-templated synthesis of CdS nanotubes in aqueous solution at room temperature. New Journal of Chemistry, 2002, 26, 1440-1442. | 2.8 | 38 |
| 390 | Synthesis of rod-, twinrod-, and tetrapod-shaped CdS nanocrystals using a highly oriented solvothermal recrystallization technique. Journal of Materials Chemistry, 2002, 12, 748-753. | 6.7 | 192 |
| 391 | Aqueous solution route to nanocrystalline HgE (E=S, Se, Te). Journal of Materials Science Letters, 2002, 21, 1657-1659. | 0.5 | 6 |
| 392 | Solid-state room-temperature route to silver composite nanowires. Journal of Materials Science Letters, 2002, 21, 1737-1738. | 0.5 | 1 |
| 393 | Microtubes and balls of amorphous phosphorus nitride imide (HPN2) prepared by a benzene-thermal method. Chemical Communications, 2001, , 469-470. | 4.1 | 9 |
| 394 | A Solution Low-Temperature Route to MoS2Fiber. Chemistry of Materials, 2001, 13, 6-8. | 6.7 | 53 |
| 395 | Cu5.5FeS6.5 nanotubesââ,¬â€a new kind of ternary sulfide nanotube. New Journal of Chemistry, 2001, 25, 1359-1361. | 2.8 | 18 |
| 396 | Antimony sulfide tetragonal prismatic tubular crystals. Journal of Materials Chemistry, 2001, 11, 257-259. | 6.7 | 25 |

| # | Article | IF | CITATIONS |
|-----|---|------|-----------|
| 397 | Metastable MnS Crystallites through Solvothermal Synthesis. Chemistry of Materials, 2001, 13, 2169-2172. | 6.7 | 146 |
| 398 | Ethanolthermal synthesis to \hat{I}^3 -Cul nanocrystals at low temperature. Journal of Materials Science Letters, 2001, 20, 1865-1867. | 0.5 | 31 |
| 399 | Preparation and characterization of CuInS ₂ nanorods and nanotubes from an elemental solvothermal reaction. Journal of Materials Research, 2001, 16, 2805-2809. | 2.6 | 42 |
| 400 | A novel twoÂstep radiation route to PbSe crystalline nanorods. Journal of Materials Chemistry, 2001, 11, 518-520. | 6.7 | 24 |
| 401 | Single-step synthesis of nanocrystalline CdS/polyacrylamide composites by Î ³ -irradiation. Journal of Materials Science, 2000, 35, 285-287. | 3.7 | 18 |
| 402 | Synthesis of short CdS nanofiber/poly(styrene-alt-maleic anhydride) composites using γâ€irradiation. Journal of Materials Chemistry, 2000, 10, 329-332. | 6.7 | 22 |
| 403 | Hydrothermal Evolution of the Thioureaâ^'Cerium(III) Nitrate System:Â Formation of Cerium Hydroxycarbonate and Hydroxysulfate. Inorganic Chemistry, 2000, 39, 4380-4382. | 4.0 | 23 |
| 404 | Syntheses, Structures and Magnetic Behaviors of Di- and Trinuclear Pivalate Complexes Containing Both Cobalt(II) and Lanthanide(III) Ions. Inorganic Chemistry, 2000, 39, 4165-4168. | 4.0 | 37 |
| 405 | Lowâ€Temperature Synthesis of Nanocrystalline Titanium Nitride via a Benzene–Thermal Route. Journal of the American Ceramic Society, 2000, 83, 430-432. | 3.8 | 72 |
| 406 | A solvothermal reaction route for the synthesis of CuFeS ₂ ultrafine powder. Journal of Materials Research, 1999, 14, 3870-3872. | 2.6 | 6 |
| 407 | A Novel Low-Temperature Synthetic Route to Crystalline Si3N4. Advanced Materials, 1999, 11, 653-655. | 21.0 | 41 |
| 408 | A Solvothermal Elemental Reaction To Produce Nanocrystalline ZnSe. Inorganic Chemistry, 1998, 37, 2844-2845. | 4.0 | 93 |
| 409 | A Reduction-Pyrolysis-Catalysis Synthesis of Diamond. , 1998, 281, 246-247. | | 117 |
| 410 | Structural variation and recovery of superconductivity by Ca substitution in Y0.4Pr0.6Bs2?x Ca x Cu3. Journal of Superconductivity and Novel Magnetism, 1996, 9, 89-91. | 0.5 | 2 |
| 411 | Low-temperature deposition of ultrafine rutile TiO2 thin films by the hydrothermal method. Physica Status Solidi A, 1996, 156, 381-385. | 1.7 | 17 |
| 412 | Preparation of Nanocrystalline Cadmium Powder by the γ-Radiation Method. Materials Transactions, JIM, 1995, 36, 80-81. | 0.9 | 6 |
| 413 | Oxygen Content, Crystal Structure, and Superconductivity in YSr2Cu2.75Mo0.25O7+l´. Physica Status Solidi (B): Basic Research, 1995, 189, 171-175. | 1.5 | 2 |
| 414 | Study of the Raman spectrum of nanometer SnO2. Journal of Applied Physics, 1994, 75, 1835-1836. | 2.5 | 183 |

Υίται Qian

| # | Article | IF | CITATIONS |
|-----|--|-----|-----------|
| 415 | Effects of ionic radius on structure and superconductivity for high-Tc oxide superconductors. Physica Status Solidi A, 1992, 130, 415-420. | 1.7 | 6 |
| 416 | Structural Characteristics of High Tc Superconducting Oxide in (Bi,Pb)-Sr-Ca-Cu-O System. Molecular Crystals and Liquid Crystals Incorporating Nonlinear Optics, 1990, 184, 401-408. | 0.3 | 0 |
| 417 | Superconducting Behavior of Bi _{1.5} Pb _{0.5} Ca ₂ Sr ₂ Cu ₃ O _y at Low Magnetic Field. Physica Status Solidi (B): Basic Research, 1989, 154, K51. | 1.5 | 0 |
| 418 | SUPERCONDUCTIVITY ASSOCIATED WITH THE GRANULAR STRUCTURE IN Ba2YCu3O7â~'δ. Modern Physics Letters B, 1988, 02, 1011-1015. | 1.9 | 0 |
| 419 | TRANSPORT PROPERTIES IN SINGLE PHASE SUPERCONDUCTOR Ba2YCu3O9â^î´. International Journal of Modern Physics B, 1987, 01, 485-489. | 2.0 | 0 |
| 420 | Enhanced Hydrogen Evolution Catalysis from hierarchical nanostructure Coâ€P@CoMoâ€P electrode. European Journal of Inorganic Chemistry, 0, , . | 2.0 | 1 |
| 421 | Constructing Complementary Catalytic Components on Co ₄ N Nanowires to Achieve Efficient Hydrogen Evolution Catalysis. Advanced Energy and Sustainability Research, 0, , 2100219. | 5.8 | 5 |
| 422 | Polydimethylsiloxane functionalized separator for a stable and fast lithium metal anode. CrystEngComm, 0, , . | 2.6 | 0 |